

difficult to assess an upper limit of  $\mu\tau$  for the level in question. In the case of level  $P_2$  in the  $n$ -type sample, the value given is based on the assumption that the low-energy tail of the spectrum is associated with this level.

For level  $N_2$ ,  $\sigma_h$  is larger than  $\sigma_e$  by orders of magnitude, indicating that  $N_2$  is an acceptor level. Level  $P_1$  has a fairly large  $\sigma_h$ ; this is consistent with the interpretation that it is an acceptor level. Level  $N_1$  is close to the conduction band and its capture cross section for electrons is not too low. It is reasonable to assume that

it is a donor level. It is difficult to postulate about the nature of level  $P_2$  from the available data.

The identification of level  $P_1$  with a level found in unbombarded samples shows directly the importance of lattice defects in determining the normal carrier concentration in GaSb. The level is probably associated with lattice vacancies, either commonly postulated Ga vacancies or Sb vacancies, as a simple interpretation of the work of Effer and Etter<sup>6</sup> would indicate. Neither type of defects can be convincingly ruled out as capable of giving acceptor levels.

## Polarization of Silver Nuclei in Metallic Iron and Nickel\*

G. A. WESTENBARGER† AND D. A. SHIRLEY

*Department of Chemistry and Lawrence Radiation Laboratory,  
University of California, Berkeley, California*

(Received 12 October 1964)

Nuclei of  $\text{Ag}^{104}$  and  $\text{Ag}^{110m}$  were polarized at temperatures between 0.0105 and 0.97°K, employing the large hyperfine magnetic fields induced at the nuclei of silver atoms dissolved in iron and in nickel. The temperature and angular dependences of  $\gamma$ -ray angular distributions were used to determine the magnitudes of the hyperfine structure constants. Nonconservation of parity in beta decay was used to determine the signs of the internal fields, using germanium detectors to count positrons from  $\text{Ag}^{104}$  and electrons from  $\text{Ag}^{110m}$ . The hyperfine fields were found to be negative in both iron and nickel. Analysis of the  $\gamma$ -ray data on one-hour  $\text{Ag}^{104}$  yielded approximate values for the internal fields:  $H_i(\text{Ag in Fe}) = -350 \pm 100$  kG,  $H_i(\text{Ag in Ni}) = -108 \pm 30$  kG. Cobalt-60  $\gamma$ -ray thermometry was used, and the problems of thermometry at 0.01°K are discussed. Nuclear spins of four levels in  $\text{Cd}^{110}$  were determined unambiguously, confirming earlier work, which was re-interpreted where necessary. The energy levels (spins) are 2162 keV (3+), 2219 keV (4+), 2479 keV (6+), 2926 keV (5+). The 1384-keV  $\gamma$  ray in  $\text{Cd}^{110}$  was found to be (91.7±2.8)% magnetic dipole and (8.3±2.8)% electric quadrupole. The 1505-keV  $\gamma$  ray was (78.9±4.8)% magnetic dipole and (21.1±4.8)% electric quadrupole. An approximate value of  $+2.9 \pm 1.3$  nm was determined for the nuclear moment of  $\text{Ag}^{110m}$ .

### I. INTRODUCTION

SINCE the discovery by Samoilov, Sklyarevskii, and Stepanov<sup>1</sup> that large hyperfine magnetic fields are induced at nuclei of atoms dissolved in iron, several such fields have been measured. No quantitative theory for these induced fields exists; in fact even an unambiguous qualitative understanding is not presently available. It seems important, therefore, to make systematic measurements of induced fields at nuclei of various elements throughout the periodic table, with emphasis on those systems that are most accessible to theoretical study. With this aim we have performed nuclear orientation experiments on silver atoms in iron and nickel lattices. This study complements measurements on the other group IB metals, copper<sup>2,3</sup> and gold.<sup>4,5</sup>

\* Work supported by the U. S. Atomic Energy Commission.

† Present address: Department of Chemistry, Ohio University, Athens, Ohio.

<sup>1</sup> B. N. Samoilov, V. V. Sklyarevskii, and E. P. Stepanov, *Zh. Eksperim. i Teor. Fiz.* **36**, 644 (1959) [English transl.: *Soviet Phys.—JETP* **9**, 448 (1959)].

<sup>2</sup> T. Kushida, A. H. Silver, Y. Koi, and A. Tsujimura, *J. Appl. Phys. Suppl.* **33**, 1079 (1962).

The theory and applicability of the technique are discussed in Sec. II. The apparatus is described in Sec. III. Section IV deals with the important subject of thermometry. In Sec. V nuclear results are derived, and in Sec. VI the induced magnetic fields at Ag nuclei in Fe and Ni are deduced.

### II. THEORY OF THE MEASUREMENTS

The general theory of nuclear orientation has been formulated by several authors.<sup>6-8</sup> Only those parts of the theory that are applicable to the polarization of nuclei in ferromagnets are summarized here.

<sup>3</sup> K. Asayama, S. Kobayashi, and J. Itoh, *J. Phys. Soc. Japan* **18**, 458 (1963).

<sup>4</sup> R. W. Grant, Morton Kaplan, D. A. Keller, and D. A. Shirley, *Phys. Rev.* **133**, A1062 (1964).

<sup>5</sup> L. D. Roberts and J. O. Thomson, *Phys. Rev.* **129**, 664 (1963).

<sup>6</sup> W. J. Huiskamp and H. A. Tolhoek, in *Progress in Low Temperature Physics III*, edited by C. J. Gorter (North-Holland Publishing Company, Amsterdam, 1961), p. 333.

<sup>7</sup> H. A. Tolhoek and J. A. M. Cox, *Physica* **19**, 101 (1953).

<sup>8</sup> R. J. Blin-Stoyle and M. A. Grace, in *Handbuch der Physik*, edited by S. Flügge (Springer-Verlag, Berlin, 1957), Vol. 42, p. 556.

Polarization of nuclei in a ferromagnet arises through interaction of the nuclear magnetic dipole moment  $\mathbf{u}$  with a hyperfine magnetic field  $\mathbf{H}_i$ . The sense and direction of  $\mathbf{H}_i$  are fixed in space by a small polarizing field  $\mathbf{H}_e$  applied externally. The orders of magnitude of  $\mathbf{H}_i$  and  $\mathbf{H}_e$  are  $10^5$ – $10^6$  and  $10^3$  G, respectively. Thus,  $\mathbf{H}_e$  establishes a quantization axis along the resultant field,  $\mathbf{H}_r = \mathbf{H}_i + \mathbf{H}_e'$ . Here  $\mathbf{H}_e'$  is the external field modified in the usual way by the Lorentz field and the demagnetizing field. It is important to note that  $\mathbf{H}_r$  need not be parallel or antiparallel to  $\mathbf{H}_e$ .

The Hamiltonian governing orientation of the spin system is

$$\mathfrak{H} = -\mathbf{u} \cdot \mathbf{H}_r = -g\beta_N M H_r. \quad (1)$$

Here  $g$  is the nuclear  $g$  factor,  $\beta_N$  is the nuclear magneton, and  $M$  is the component of nuclear spin along the quantization axis. At equilibrium the spins are distributed according to the statistical population function

$$W(M) = Z^{-1} \exp(-g\beta_N M H_r / kT), \quad (2)$$

where  $Z$  is the partition function. Substantial nuclear orientation occurs when  $g\beta_N H_r / kT$  is of the order of unity or larger. For  $g=1$  this requires that  $H_r/T$  be  $2.8 \times 10^7$  G/deg. Thus, temperatures of the order of  $10^{-2}$  °K are required for orientation even in most of the large internal fields available in ferromagnets.<sup>9</sup>

The degree of orientation is most conveniently given by the usual statistical tensors<sup>8</sup>

$$B_k = (2I+1)^{1/2} \sum_m (-)^{I-M} C(I I k; M - M) W(M), \quad (3)$$

and the angular distribution of radiation following the decay of oriented nuclei can be written

$$W(\theta) = \sum_{k=0}^{\lambda} B_k U_k F_k P_k(\cos\theta). \quad (4)$$

Here  $\theta$  is the angle between the propagation direction of the radiation and the quantization axis. The functions  $U_k$  and  $F_k$  are discussed by Blin-Stoyle and Grace.<sup>8</sup> Angular momentum triangle conditions set an upper limit  $\lambda$  on the rank of nonvanishing tensors. For the work discussed here no radiation quanta carried more than two units of angular momentum from the nucleus; therefore  $\lambda$  was 4. Because parity is conserved in electromagnetic interactions, only the  $k=0, 2, 4$  terms contributed to the angular distribution of gamma radiation. Parity is not conserved in beta decay, and the  $k=0, 1$  terms were important in the angular distributions of beta particles. Higher  $k$  gave no contributions to the beta-particle distributions from  $\text{Ag}^{104}$  and  $\text{Ag}^{110m}$  because<sup>10</sup> the transitions were allowed.<sup>11</sup>

<sup>9</sup> A few rare-earth metals have larger fields ( $\sim 10^7$  G), and must be excepted from this statement.

<sup>10</sup> Hans A. Weidenmüller, *Rev. Mod. Phys.* **33**, 574 (1961).

<sup>11</sup> H. W. Taylor and W. R. Frishen, *Phys. Rev.* **114**, 127 (1959).

A careful determination of the temperature dependence of  $B_2 U_2 F_2$ , together with knowledge of  $U_2 F_2$ , yields  $B_2(T)$  directly. By combining  $B_2(T)$  with Eqs. (2) and (3), one obtains  $|\mu H_r|$ . From  $\gamma$ -ray directional distributions alone one cannot obtain the sign of this product, because there are no odd  $k$  terms in Eq. (4). ( $\gamma$ -ray circular polarization measurements do yield the sign.) If enough is known about the observed beta transition, a determination of the sign of the “forward-backward” beta asymmetry yields the sign of the  $\mu H_r$  product. For a pure Gamow-Teller transition ( $\text{Ag}^{104}$ ) with  $I(\text{initial})=I(\text{final})+1$ , the angular distribution is given by<sup>6,8</sup>

$$W(\theta, e^\pm) = 1 \pm [(I+1)/3I]^{1/2} (v/c) B_1 \cos\theta. \quad (5)$$

For  $\Delta I=0$  and a Gamow-Teller transition, the distribution is given by

$$W(\theta, e^\pm) = 1 \pm [1/3I(I+1)]^{1/2} (v/c) B_1 \cos\theta. \quad (6)$$

In both (5) and (6)  $v$  is the electron velocity and  $\theta$  is taken as zero in the positive sense along the quantization axis.

### III. APPARATUS

It seems very probable that the orientation, by induced hyperfine fields, of nuclei of atoms dissolved in iron and other magnetic lattices will be exploited considerably in the near future. The cryogenic techniques required for these experiments are somewhat demanding and not generally known. Several features of our apparatus, including its ability to cool radioactive specimens to 0.0105°K and to keep them in this temperature range for hours, are unique. Thus we describe the essential points of this apparatus below.

The helium bath could be pumped to 0.97°K by the use of a 1250 cubic feet/minute mechanical booster pump. At this temperature the equilibrium adsorption pressure of  $\text{He}^4$  heat-exchange gas is very low and a cryostat pressure of  $10^{-6}$  mm Hg could be obtained by only a few minutes of pumping. The cryostat was made of glass to facilitate inductance measurements and to provide a clean surface; it was joined to the vacuum system by a Housekeeper seal and soft solder. Care was taken to make the entire exchange-gas vacuum system as clean as possible, using welded stainless-steel tubing wherever feasible.

The iron-alloy sample, of approximate dimensions 4 mm  $\times$  2 mm  $\times$  0.1 mm, was soft-soldered to a laminated fin assembly consisting of 25 pieces of 0.005-in. Cu foil, silver-soldered together at the top. The foils were cut with a protrusion to support the sample at the top end; the bottom end of each foil made contact with a “chrome alum-glycerine” slurry. The slurry was prepared by stirring powdered chromium potassium sulfate with a 1:1 by volume mixture of a saturated aqueous solution of chromium potassium sulfate and glycerine. The usual proportions were 12 g of salt to 5 g of 1:1 mixture, but

the consistency of the slurry determined the exact composition in each case. The slurry was carefully spread onto both sides of each fin and the assembly was placed into a glass container which was in turn suspended by spring-loaded nylon threads in the cryostat vacuum space. The protrusion holding the sample was inserted into (but did not touch) a  $\frac{3}{8}$ -in.-long by  $\frac{1}{2}$ -in.-o.d. by  $\frac{3}{8}$ -in.-i.d. niobium metal tube. At 1°K this superconducting tube trapped over 2000 G during the demagnetization, thus polarizing the sample. The total contact area of copper fins and slurry was 800 cm<sup>2</sup>, and new slurry was made for each run.

#### IV. THERMOMETRY

Thermometry in the 10<sup>-2</sup> °K temperature range is in a very primitive state. Most "magnetic temperature scales" for paramagnetic salts yield absolute temperatures with quoted accuracies of only about 10%, and various evidence obtained by nuclear orientation measurements in this laboratory indicates that these estimated errors are by no means too large. Thus, while a  $T-T^*$  correlation for chrome alum is available, it would be very unattractive to base quantitative results on this correlation.

There are additional objections against using only magnetic thermometry. Thermal equilibrium between sample and slurry is not possible because an appreciable fraction of the total heat leak (including radioactive heating) comes in through the sample and fin assembly. The shape of the paramagnetic slurry, partitioned by the copper fins, was such as to preclude an exact demagnetization-factor correction. Finally, the instability of chrome alum itself casts doubt on magnetic thermometry employing it.

We elected to measure temperatures "internally" by incorporating Co<sup>60</sup> into the sample and using the angular distributions of the 1.173- and 1.333-MeV  $\gamma$  rays following the decay of oriented Co<sup>60</sup> to determine the temperature. This procedure is thermodynamically imperfect in the sense of not being completely empirical. It is, however, valid to the extent that the Hamiltonian governing the orientation of Co<sup>60</sup> nuclei in iron is known. This Hamiltonian has the form of Eq. (1), with  $H_i = -289.7$  kG,<sup>12</sup> and  $H_e = +2.3$  kG. The nuclear moment of Co<sup>60</sup> has the value  $+3.80$  nm.<sup>13</sup> The absolute temperature is contained implicitly in the formalism of Sec. II.

Gamma-ray thermometry has been used before,<sup>14-16</sup> usually to compare nuclear moments. It should be emphasized that such a comparison is possible only if the temperature of the specimen is homogeneous and if the spin Hamiltonian of the "standard" isotope and

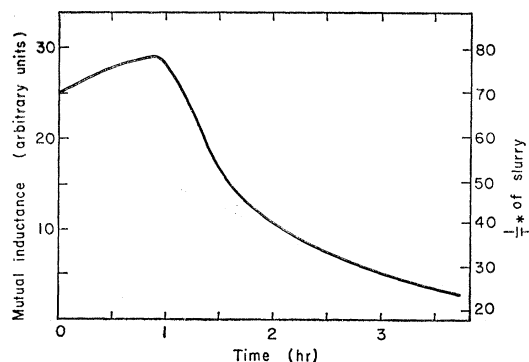


FIG. 1. Warm-up curve for chrome-alum slurry and fin assembly. The maximum susceptibility occurs just below the Curie temperature. Note that after 3.8 h the slurry has warmed up only to a  $1/T^*$  of 23. This corresponds to an absolute temperature of 0.02°K.

the form of the spin Hamiltonian of the isotope to be investigated are known.

If the appropriate criteria have been met, we believe that it is both theoretically valid and experimentally feasible to use nuclear orientation to establish a primary temperature scale in the 0.01°K range, with an absolute accuracy as high as 1%. This applies both to experiments of the type reported here and to ionic crystals, and it would constitute a tenfold improvement over the best accuracy presently available.

Figure 1 shows a "warming curve" for a well-insulated chrome alum slurry and fin assembly. The susceptibility maximum accompanying the Curie point of chrome alum (at 0.0115°K)<sup>17</sup> is clearly visible, and it comes one hour after demagnetization. In the experiments reported here this type of warming curve served as a criterion of good apparatus performance.

Temperatures obtained from the Co<sup>60</sup>  $\gamma$ -ray thermometer and the magnetic thermometer are compared

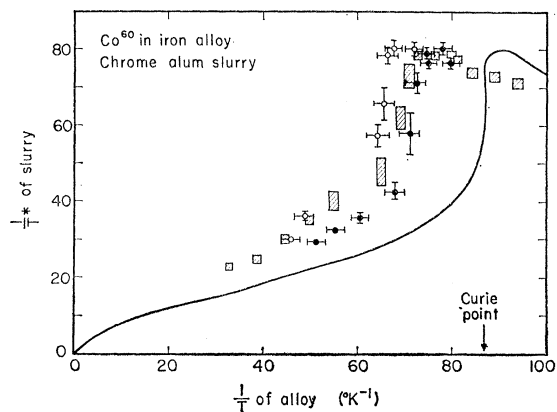


FIG. 2. Plot of alloy temperature against magnetic temperature of salt slurry. Solid curve is the salt temperature, based on the  $T-T^*$  correlation. Three sets of points give temperatures obtained from Co<sup>60</sup> thermometer in three different assemblies.

<sup>12</sup> Y. Koi, A. Tsujimura, T. Hihara, and T. Kushida, J. Phys. Soc. Japan **16**, 1040 (1961).

<sup>13</sup> W. Dobrowolski, R. V. Jones, and C. D. Jeffries, Phys. Rev. **101**, 1001 (1955).

<sup>14</sup> J. C. Wheatley, D. F. Griffing, and R. D. Hill, Phys. Rev. **99**, 334 (1955).

<sup>15</sup> R. W. Bauer and M. Deutsch, Phys. Rev. **117**, 519 (1960).

<sup>16</sup> N. J. Stone and B. G. Turrell, Phys. Letters **1**, 39 (1962).

<sup>17</sup> J. M. Daniels and N. Kurti, Proc. Roy. Soc. (London) **A221**, 243 (1954).

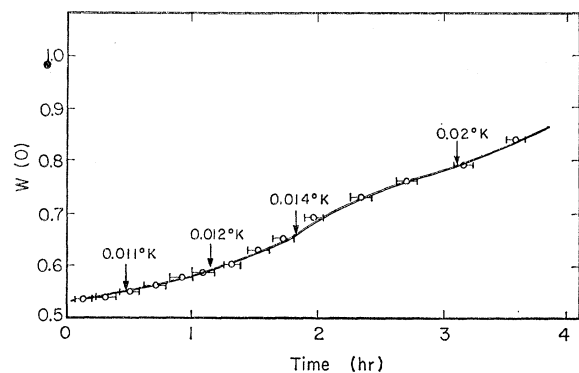


FIG. 3. Magnitude of  $W(0)$  for  $\text{Co}^{60}$  in iron as a function of time after end of demagnetization. This run was used for Fig. 1 and data from it appear as shaded rectangles in Fig. 2.

in Fig. 2. The  $\text{Co}^{60}$   $\gamma$ -ray intensity for the run that was used in Fig. 1 and that appeared in Fig. 2 is plotted against time in Fig. 3. The lowest  $\gamma$ -ray temperature was  $0.0105^\circ\text{K}$ , substantially below the accepted Curie point of  $0.0115^\circ\text{K}$ . However, the sample temperature was  $0.0115^\circ\text{K}$  50 min after demagnetization, when the salt in the slurry was at the susceptibility maximum. If the salt and sample were in thermal equilibrium at this point, this agreement would support the established Curie point. We can say with confidence that the Curie point of chrome alum is *no higher* than  $0.0115^\circ\text{K}$ .

In the early stages of this work a value of  $-80$  kG for the internal field of Co in Ni was used and the nickel data did not agree with the iron data. The Co in Ni thermometer consistently suggested that temperatures in the  $1/T \cong 120$  range were being reached. The  $-80$ -kG internal field had been obtained by a rather questionable extrapolation of heat capacity data.<sup>18</sup> After many experiments had established our confidence in the  $\text{Co}^{60}$  thermometer, we abandoned this internal field value in favor of a value of  $-120$  kG which we determined and were prepared to report. A NMR measurement then became available,<sup>19</sup>  $H_i = -112.7$  kG at  $27.4^\circ\text{C}$ . This may be corrected to  $-123$  kG at  $0^\circ\text{K}$ , in very good agreement with our result.

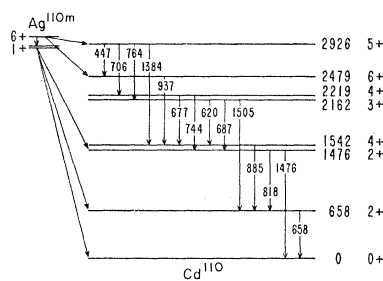


FIG. 4. Decayscheme of  $\text{Ag}^{110m}$ .

<sup>18</sup> V. Arp, D. Edmonds, and R. Petersen, Phys. Rev. Letters **3**, 212 (1959).

<sup>19</sup> R. C. LaForce (private communication).

## V. NUCLEAR RESULTS

The energy-level scheme of  $\text{Cd}^{110}$ , as deduced from the decay of  $\text{Ag}^{110m}$ , is shown in Fig. 4. Most of the information given there was taken from electron and  $\gamma$ -ray spectroscopy measurements and angular correlation work in the literature.<sup>11,20-26</sup> The nuclear orientation results that we report here serve to establish some spins uniquely, to confirm others, and (especially in conjunction with the angular correlation data) to determine multipolarity mixtures in mixed  $M1$ - $E2$  transitions with good accuracy.

The approach used in analyzing the data was to determine  $B_2U_2F_2$  [the coefficient of  $P_2$  in Eq. (4)] with high precision for each  $\gamma$  ray, where possible. The spectrum is complex (Fig. 5), and several  $\gamma$  rays are unresolved. Fortunately the energies and approximate relative intensities are available.<sup>21,24,26</sup> The analysis was

TABLE I. Experimental values of  $B_2U_2F_2$  for  $\gamma$  rays from  $\text{Ag}^{110m}$  nuclei oriented in iron.

Energy <sup>a</sup> (keV)	Relative intensity, <sup>b</sup> with errors in parentheses	$B_2U_2F_2$ at $0.111^\circ\text{K}$ (errors in parentheses)
447	6.4(0.8)	<0
620	3.9(0.5)	> -0.3
658	100	< -0.215 <sup>c</sup>
677	10(1)	} >0
687	7(1)	
706	19(2)	> +0.30
744	6(2)	...
764	24(2)	-0.30(2)
818	8.5(1)	...
885	76(4)	-0.324
937	33(2)	-0.31(1)
1384	27(2)	+0.680(10)
1476	5.5(1)	} +0.480(6)
1505	14(1)	
1561	1.3(0.2)	

<sup>a</sup> From Refs. 25 and 26.

<sup>b</sup> From Refs. 21 and 24.

<sup>c</sup> The value  $-0.215$  includes contributions from the 620-, 677-, and 687-keV transitions.

necessarily implicit, and the  $B_4U_4F_4$  term, which was always small, was treated as a correction. The background correction for lower energy  $\gamma$  rays, which arises largely from Compton scattering of higher energy  $\gamma$  rays, presents a very difficult problem. One cannot, for example, assume that this background is isotropic, as it certainly is not. The anisotropy of Compton-scattered radiation is not equal to that of the corresponding

<sup>20</sup> E. G. Funk, Jr., and M. L. Wiedenbeck, Phys. Rev. **112**, 1247 (1958).

<sup>21</sup> B. S. Dzelepov and N. N. Zhurkovsky, Nucl. Phys. **6**, 655 (1958).

<sup>22</sup> H. W. Taylor and S. A. Scott, Phys. Rev. **114**, 121 (1959).

<sup>23</sup> A. C. Knipper, Proc. Phys. Soc. (London) **71**, 77 (1958).

<sup>24</sup> N. M. Anton'eva, A. A. Bashilov, and E. E. Kulakovskii, Zh. Eksperim. i Teor. Fiz. **37**, 1479 (1959) [English transl.: Soviet Phys.—JETP **10**, 1063 (1960)].

<sup>25</sup> Toshio Katoh and Yasukaga Yoshizawa, Nucl. Phys. **32**, 5 (1962).

<sup>26</sup> T. Suter, P. Reyes-Suter, W. Schever, and E. Aasa, Nucl. Phys. **47**, 251 (1963).

photopeak, either (as it would very nearly be if scattering occurred only in the NaI crystal); in fact it may even have the opposite sign, because of the  $\gamma$ -ray polarization.<sup>27</sup> An estimate of the experimental background anisotropy may be obtained from Fig. 6, in which the intensity at  $\theta=0$  and  $T=0.01^\circ\text{K}$  is plotted against photon energy. The photopeaks that will yield the most reliable anisotropies are those at the highest energies, in this case the 885-, 937-, 1384-, and 1505-keV peaks.

In Table I the average values of  $B_2U_2F_2$  for several peaks are set out. These were obtained by averaging data for each peak from several runs for which the reciprocal temperatures were near the average value of  $90 \text{ deg}^{-1}$ . We note that the values of  $B_2U_2F_2$  have relative precisions in some cases far better than their absolute accuracies. Thus, the figure  $1/T=90 \text{ deg}^{-1}$  is a nominal value, known to no better than 2%. We discuss the peaks separately below.

*The 885-keV peak.* This  $\gamma$  ray is known to have  $E2$  multipolarity and has a well-established position in the decay scheme. We use it as our internal standard of comparison to determine  $F_2$ 's for the other  $\gamma$  rays (leading to a 5% correction noted at the end of this section). For the spin-multipolarity combination  $4(E2)2$ , we have  $F_2(885)=-0.448$ . The  $U_2$  for this transition can be calculated from the spins, multiplicities, and relative intensities of preceding transitions (although this is a "bootstrap" operation in that the resulting quantities will be used to determine these spins and multiplicities,  $U_2$  is a slowly varying function of these parameters, and it is not possible, in this case, to converge on a spurious solution by iteration). By this procedure we find  $U_2(885)=0.763\pm 0.034$ . Comparison with Table I yields  $B_2=+0.95\pm 0.05$ . The quoted error arises from uncertainties in the temperature scale, background corrections, and the error in the determination of  $U_2(885)$ . At the end of this section, this  $B_2$  will be revised downward by 5% to bring it into better agreement with other angular distribution data.

*The "658-keV" peak.* This peak includes the 620- and 677-keV  $\gamma$  rays as well as its main component, the 658-keV  $\gamma$  ray. The value of  $B_2U_2F_2$  for the 658-keV  $\gamma$  ray should, from the decay scheme, be  $+0.964\pm 0.041$  times that of the 885-keV  $\gamma$  ray. From Table I, the ratio  $B_2U_2F_2$  ("658 peak")/ $B_2U_2F_2$  (885) is in fact  $+0.66\pm 0.02$ . This lower ratio must arise from contributions to the "658 peak" of the 620- and 677-keV  $\gamma$  rays, which must have values of  $B_2U_2F_2$  quite different from that of the 658-keV  $\gamma$  ray. Detailed analysis gave the limits on  $B_2U_2F_2$  (620) and  $B_2U_2F_2$  (677) that are listed in Table I.

*The 1384-keV peak.* From Table I we find  $U_2F_2(1384)/U_2F_2(885)=-2.10\pm 0.05$ . For a pure Gamow-Teller transition from the  $6+$  state in  $\text{Ag}^{110m}$  to the 2925-keV level, we have  $U_2=+0.97$ . A  $6+$  spin and parity com-

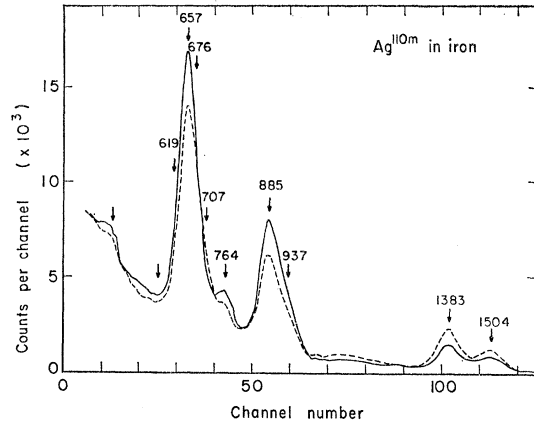


FIG. 5. Gamma-ray spectrum of  $\text{Ag}^{110m}$  obtained along polarizing axis with the iron alloy cooled to near  $0.01^\circ\text{K}$  (dashed curve) and at about  $1^\circ\text{K}$  (solid curve).

bination for this level is immediately ruled out by the sign of  $B_2U_2F_2(1383)$ . Thus we find

$$F_2^L(1384)=+0.74\pm 0.05,$$

where  $L$  denotes last in a cascade.<sup>28</sup> The amplitude mixing ratio,  $\delta(E2/M1)$ , for this cascade is thus either  $\delta^L=-0.273\pm 0.027$  or  $\delta=-2.21\pm 0.15$ . This latter possibility is easily ruled out by the angular correlation data, which are in reasonable agreement for the former value. Actually the quoted error limits for the various experiments do not quite overlap, but the errors quoted for the angular correlation data are too small, considering that little or no correction was made for interfering radiations for which the intensities were then unknown. The angular correlation results and the values of  $F_2^F(1384)$  obtained from the available angular correlation data are listed, along with the derived values of  $\delta^F$ , in Table II. We note that by definition<sup>28,29</sup>  $\delta^F=-\delta^L$ . The data are all consistent with the 1384-keV transition being of  $(8.3\pm 2.8)\%$  dipole and  $(91.7\pm 2.8)\%$  quad-

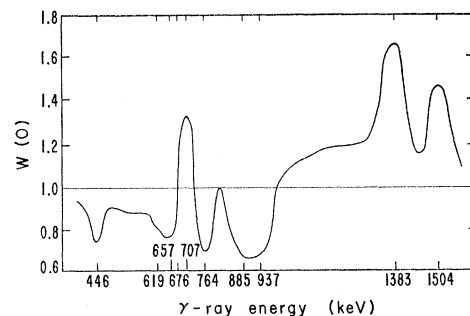


FIG. 6. Plot of  $W(0)$  versus photon energy for  $\text{Ag}^{110m}$  nuclei oriented at  $10^{-2}\text{K}$  in iron. Several unresolved  $\gamma$  rays are clearly anisotropic.

<sup>27</sup> J. N. Haag, D. A. Shirley, and David H. Templeton, Phys. Rev. **129**, 1601 (1963).

<sup>28</sup> G. A. Westenbarger and D. A. Shirley, Phys. Rev. **123**, 1812 (1961).

<sup>29</sup> L. C. Biedenharn and M. E. Rose, Rev. Mod. Phys. **25**, 729 (1953).

TABLE II. Angular distribution coefficients and derived amplitude mixing ratios for the 1384-keV  $\gamma$  ray in  $\text{Cd}^{110}$ .

$F_2^a$	Type <sup>b</sup>	$\delta(E2/M1)^{a,c}$	Reference
+0.74(5)	<i>L</i>	-0.274(34)	This work
+0.634(16)	<i>F</i>	+0.341(12)	11
+0.688(29)	<i>F</i>	+0.387(30)	20
+0.643(27)	<i>F</i>	+0.349(22)	23

<sup>a</sup> Errors in last place are given in parentheses.

<sup>b</sup> The "first" and "last" in cascade classification is discussed in Ref. 28.

<sup>c</sup> By definition,  $\delta^F = -\delta^L$ .

rupole multipolarity and proceeding from a 5+ state at 2925 keV to a 4+ state at 1542 keV in  $\text{Cd}^{110}$ .

*The 1505-keV peak.* This peak is complex; it consists of  $\gamma$  rays at 1476, 1505, and 1561 keV, in relative intensities 5.5:14:1.3. The 1476- and 1561-keV transitions are "stretched" *E2* transitions between states of known spins. Thus their angular distribution coefficients may be calculated.

Angular correlation data are available for two cascades involving the 1505-keV transition. Taylor and Frishen studied the 764-1505-keV cascade, finding  $A_2 = -0.1627 \pm 0.0063$  and  $A_4 = -0.0031 \pm 0.0098$ . These results require  $F_2^L(1505) = +0.79 \pm 0.03$ , if no corrections are made for competing radiations. This  $F_2$  should be revised slightly upward to account for inclusion of the 1476-keV  $\gamma$  ray in the correlation, both through the 744-1476-keV cascade and through the 764-687-1476-keV cascade. We cannot assess the corrections accurately because not enough information is available, but an estimate may be made from known relative intensities, spins, and multiplicities. After this correction, we find  $F_2^L(1505) = +1.03 \pm 0.06$ . After corrections for the angular distributions of the 1476- and 1561-keV  $\gamma$  rays, our nuclear orientation data give  $F_2^L(1505) = +1.06 \pm 0.10$ , in excellent agreement.

Angular correlation data are also available, for the 1505-658-keV cascade, in which the 1505-keV  $\gamma$  ray is first in cascade. The  $A_2$ 's and derived values for  $F_2^F(1505)$  are given in Table III. We conclude that all the data are consistent only with the 1505-keV transition being a (78.9 $\pm$ 4.8)% *M1* and (21.1 $\pm$ 4.8)% *E2*, proceeding from a 3+ state at 2162 keV to a 2+ state at 658 keV.

TABLE III. Angular distribution coefficients and derived amplitude mixing ratios for the 1505-keV  $\gamma$  ray in  $\text{Cd}^{110}$ . Value adopted from overlap of allowed ranges:  $\delta^L = -0.515(75)$ .

Observed function <sup>a</sup>	Value (errors in parentheses)	Derived $F_2^b$	$\delta(E2/M1)$	Reference
$U_2 F_2(1505)$	+0.506(25)	+1.06(10)	-0.43 $>\delta^L >$ -1.32	This work
$A_2(764-1505)$	-0.1627(63)	+1.03(6)	-0.44 $>\delta^L >$ -1.29	11
$A_2(1505-658)$	-0.34(7)	+0.63(13)	+0.31 $<\delta^F <$ +0.59	23
$A_2(1505-658)$	-0.40 <sub>-0.07</sub> <sup>+0.13</sup>	+0.78(18)	+0.41 $<\delta^F <$ +4.6	20

<sup>a</sup> The measurements were made on the "1505-keV peak," which includes much of the 1476- and 1561-keV  $\gamma$  rays.

<sup>b</sup> Corrections have been made for interfering radiations, as discussed in text.

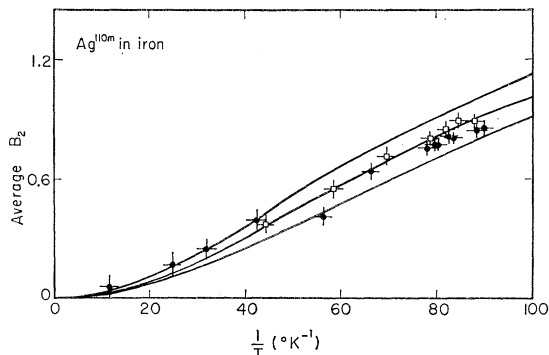


FIG. 7. Average value of  $B_2$  obtained by analysis of three  $\gamma$  rays from  $\text{Ag}^{110m}$  in iron plotted as a function of  $1/T$ . The curves were calculated by using the values of  $|\mu H|$  shown. The curves are (from the top) for  $|\mu H|$  of  $1.1 \times 10^6$ ,  $1.0 \times 10^6$ , and  $0.9 \times 10^6$  nm-G, respectively.

*The 937-keV peak.* The ratio  $U_2 F_2(937)/U_2 F_2(885) = 0.957 \pm 0.031$  leads to  $F_2(937) = -0.364 \pm 0.027$ , based on  $F_2(885) = -0.448$ ,  $U_2(885) = +0.763 \pm 0.034$ , and  $U_2(2479) = +0.90 \pm 0.03$ . This is slightly lower than the theoretical  $F_2 = -0.402$  for a 6(*Q*)4 transition, but we regard the agreement as satisfactory. The other spin possibility of 5+ for the 2479-keV level, would require an  $F_2^L$  of -0.20 to be consistent with the angular correlation data.

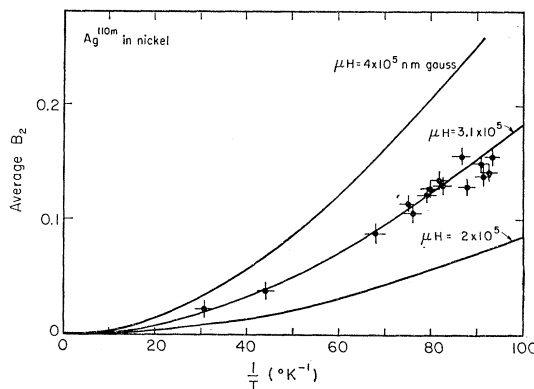


FIG. 8. Average value of  $B_2$  obtained by analysis of three  $\gamma$  rays from  $\text{Ag}^{110m}$  in nickel plotted as a function of  $1/T$ . The curves were calculated by using the values of  $\mu H$  shown.

*The 706-keV peak.* A large positive value for  $F_2^L(706)$  was observed. An  $F_2^L$  of -0.420 would be required if this transition were 5(*Q*)3. Thus, the spin of the 2219-keV level is not 3. A spin of 5 would require that the 744-keV transition be octupole, and would probably be accompanied by a beta branch from  $\text{Ag}^{110m}$ . Thus, we conclude that the 2219-keV level has spin 4.

The above arguments lead to the spins indicated in Fig. 4 for the upper levels in  $\text{Cd}^{110}$ . These assignments are unambiguous and alternative assignments would require very different angular distributions, as discussed above. At the same time the derived  $F_2$  coef-

ficients for the three transitions for which accurate data are available are not in perfect agreement. Using the 885-keV transition as a standard, as we have above, our derived values for  $F_2(937)$  and  $F_2(1384)$  are, respectively, 9 and 12% lower than the best values from angular correlation, and the "probable error" intervals do not quite overlap. The choice of the 885-keV tran-

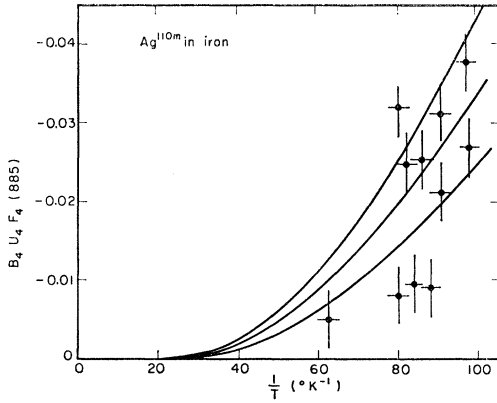


FIG. 9. Experimental  $B_4 U_4 F_4(885)$  for  $Ag^{110m}$  in iron versus  $1/T$ . Curves calculated for values of  $\mu H$  of (from top) 1.1, 1.0, and  $0.9 \times 10^6$  nm-G are shown.

sition as a standard was somewhat arbitrary, and we have therefore corrected the empirical  $B_2 U_2 F_2(885)$  upward by 5%, to obtain a most probable value, for the determination of hyperfine structure constants in the next section. This adjustment, which is within the possible error of the measurements, is entirely equivalent to taking the weighted average of the 885-, 937-, and 1384-keV data.

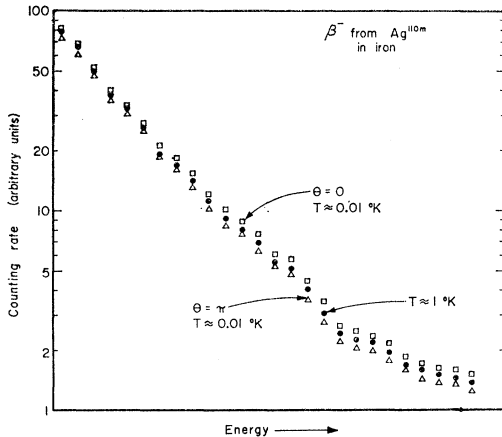


FIG. 10. Beta intensity from  $Ag^{110m}$  nuclei polarized in iron at 0.01°K, taken with and against the polarizing field, and normalizing intensity for randomly oriented nuclei at 1°K. For this 6+ to 6+ decay electrons are emitted preferentially in the direction away from the angular momentum vector. Enhancement of intensity along external field direction indicates that nuclei are oriented against this field. No energy scale is given because an accurate calibration was impossible, but this is the 400-keV region and consists almost entirely of the 530-keV branch.

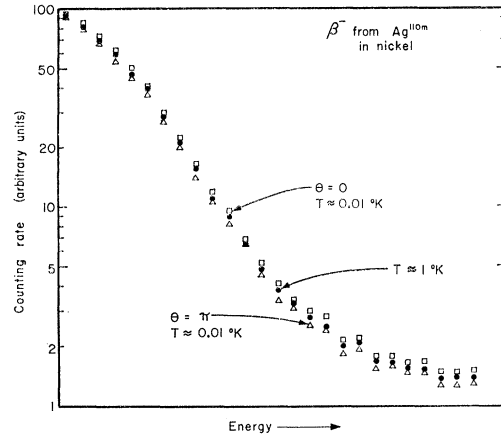


FIG. 11. Beta intensity from  $Ag^{110m}$  nuclei polarized in nickel at 0.01°K, with normalized intensity, as in Fig. 10.

VI. HYPERFINE STRUCTURE AND INTERNAL FIELDS

A. Magnitudes of the hfs Constants for  $Ag^{110m}$

From the above analysis enough was known to obtain quite consistent values of  $U_2 F_2$  for the peaks at 658, 885, 1384, and 1505 keV, especially considering the complexity of the spectrum. Samples of  $Ag^{110m}$  in iron and nickel were run, using  $Co^{60}$  as a thermometer. Values of  $B_2(T)$  were obtained, using Eqs. (2)-(4). These are compared with theoretical curves in Figs. 7

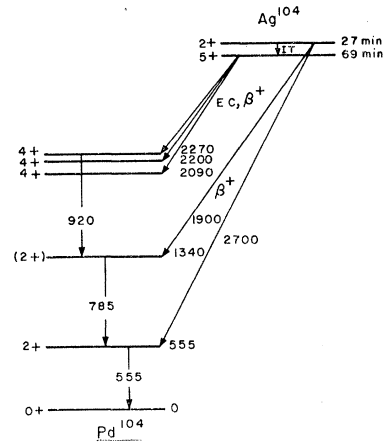


FIG. 12. Partial decay scheme for  $Ag^{104}$ , after Ref. 36.

and 8. Only the absolute values,  $|\mu H|$ , could be derived from these data. These values are

$$|\mu H| = (10.0 \pm 0.7) \times 10^5 \text{ nm-g}(Ag^{110m} \text{ in Fe}),$$

$$|\mu H| = (3.1 \pm 0.4) \times 10^5 \text{ nm-g}(Ag^{110m} \text{ in Ni}).$$

The solubility of Ag in Fe is reported<sup>30</sup> to be less than  $2 \times 10^{-3}\%$ . These experiments were run with concentrations of 10<sup>-3</sup>% and  $0.5 \times 10^{-3}\%$  to test the possibility that the Ag was incompletely dissolved. The

<sup>30</sup> A. J. Dornblatt, Trans. Electrochem. Soc. 74, 280 (1938).

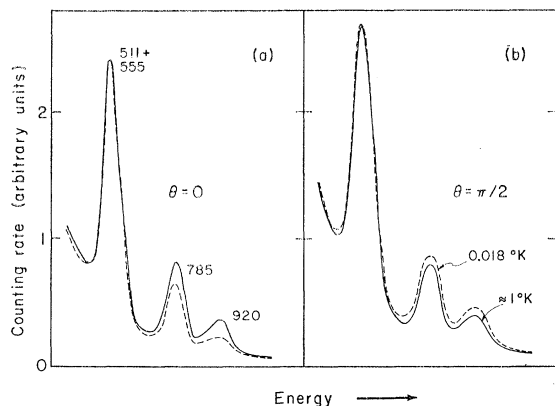


FIG. 13. Gamma-ray spectrum of  $\text{Ag}^{104}$  polarized in iron. Spectra obtained parallel and perpendicular to axis of polarization are shown. Solid curves are isotropic spectra normalized to cold counting period. Dashed curves are for  $1/T \approx 60$ .

results for these two concentrations were identical, indicating that the Ag present was all in solution in both cases (this of course implies nothing about the *equilibrium* solubility). Determination of the  $B_4U_4F_4$  (885) product provides an independent test of whether the Ag atoms are in the Fe lattice. It is easily shown that, if only a fraction of the  $\text{Ag}^{110m}$  nuclei are oriented and contribute to  $B_2U_2F_2$ , an anomalously large  $B_4U_4F_4$  will be derived from the analysis (because an erroneously low hfs constant will be calculated). The actual  $B_4U_4F_4$  (885) products indicate no such behavior (Fig. 9), and lend further support to our values for  $|\mu H|$ .

### B. Sign of $\mu H$ for $\text{Ag}^{110m}$

Determination of the sign of  $\mu H$  by the use of parity nonconservation in beta decay is a straightforward process if enough is known about the beta decay. In the decay of  $\text{Ag}^{110m}$  only the 530-keV beta branch may be conveniently studied. We used germanium beta counters, which had been shown by Navarro<sup>31</sup> to give good resolution for electrons at 1°K, to study the asymmetry of the 530-keV beta branch from polarized  $\text{Ag}^{110m}$ .

This beta branch is almost entirely a Gamow-Teller transition; Daniel *et al.*<sup>32</sup> give  $C_V M_F / C_A M_{GT} = 0.05 \pm 0.04$ . For a pure 6+ to 6+ Gamow-Teller transition  $A_-$  is  $-\frac{1}{2}$ , and we may write for the expected angular distribution of 511-keV electrons:

$$W(\theta) = 1 - 0.0775 B_1(T) \cos \theta,$$

where  $\theta$  is the angle between the polarizing field (vector) and the direction of the counter (from the source). For  $\text{Ag}^{110m}$  in Fe the  $\gamma$ -ray data yield a hfs constant that implies  $B_1 \sim 1.3$  at the lowest temperatures attainable.

<sup>31</sup> Q. O. Navarro, thesis, University of California, 1962 [Lawrence Radiation Laboratory Report No. UCRL-10362 (unpublished)].

<sup>32</sup> H. Daniel, O. Mehling, and D. Schotte, Z. Physik **172**, 202 (1963).

For  $\text{Ag}^{110m}$  in Ni this figure is  $B_1 \sim 0.7$ . Thus, asymmetries of a few percent were expected in either case. Asymmetries were found, of  $\sim 11\%$  in Fe and  $\sim 6\%$  in Ni. In both cases the  $\mu H$  product was found to be negative. Measurements were made at several electron energies and for  $\theta = 0$  and  $\pi$  in each case. Neither the energy calibration nor the scattering properties of the source were of a quality to allow a precise measurement of the asymmetry but its sign was easily determined. Typical spectra are shown in Figs. 10 and 11.

There is independent evidence from atomic-beam measurements<sup>33</sup> that the magnetic moment of  $\text{Ag}^{110m}$  is large. The largest nuclear moments are always positive (because of the proton's orbital contribution); therefore the most probable interpretation of the negative  $\mu H$  products is that  $\mu$  is positive and  $H$  negative. Negative internal fields were expected for these cases. The signs were determined directly as described below.

### C. The Hyperfine Structure of $\text{Ag}^{104}$ in Iron

After the  $\text{Ag}^{110m}$  measurements were complete we did an experiment on 69-min  $\text{Ag}^{104}$  in iron to determine the sign of the internal field directly. The spin and moments are known<sup>34,35</sup> to be  $I = 5$  and  $\mu = +4.0_{-0.1}^{+0.2}$  nm. This isomer decays<sup>36</sup> by positron emission to a 4+ state at 2270 keV in  $\text{Pd}^{104}$ . The angular distribution parameters may be calculated from the decay scheme. The  $\beta+$  branches to the known 4+ states (Fig. 12) should be pure Gamow-Teller, and the 920-keV  $\gamma$  ray should be pure  $E2$ . The short lifetime precluded highly accurate measurements, but we were able to obtain some information about the internal field from the experiment.

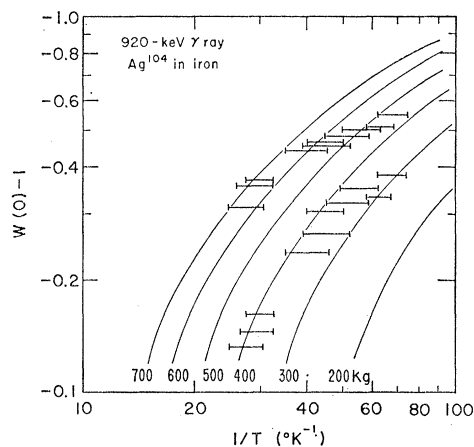


FIG. 14.  $W(0) - 1$  for 920-keV  $\gamma$  ray from  $\text{Ag}^{104}$  as a function of temperature. Two extreme values are shown at each temperature. Curves are for various values of the hyperfine field.

<sup>33</sup> W. B. Ewbank, W. A. Nierenberg, H. A. Shugart, and H. B. Sillsbee, Phys. Rev. **110**, 595 (1958).

<sup>34</sup> O. Ames, A. M. Bernstein, M. H. Brennan, R. A. Haberstroh, and D. R. Hamilton, Phys. Rev. **118**, 1599 (1960).

<sup>35</sup> O. Ames, A. M. Bernstein, M. H. Brennan, and D. R. Hamilton, Phys. Rev. **123**, 1793 (1961).

<sup>36</sup> R. K. Girgis and R. van Lieshout, Nucl. Phys. **13**, 493 (1959).



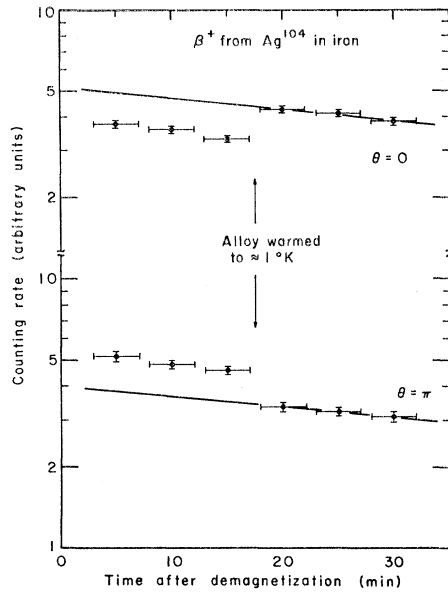


FIG. 15. Positron counting rate as a function of time after demagnetization. Note that  $\bar{W}(0) < 1$  and  $\bar{W}(\pi) > 1$  for positrons, indicating a negative hyperfine field.

The  $\text{Ag}^{104}$  was prepared by a  $(p, n)$  reaction on  $\text{Pd}^{104}$ , and the alloy contained 5% Pd. This may affect the internal field at the Ag nuclei; it is probable that the error thus introduced is small compared to other errors in the experiment.

The  $\gamma$ -ray spectra for typical "cold" and "warm" counts are shown in Fig. 13. A large source of possible error is the background correction for the 920-keV  $\gamma$  ray, which could be made only approximately in view of the incomplete knowledge of this decay. We can set extreme upper and lower limits on the internal field (Fig. 14) as follows: (a) The upper limit—The background under the 920-keV peak cannot be more than 43% of the total "warm" intensity, and the best estimate is 28%. If the extreme value of 43% is used, and the correction is made, the internal field required to fit the data varies from 700 kG at 0.03°K to 450 kG at 0.015°K. We thus find that this latter value is an upper limit for the internal field. An independent check is the fact that the small  $B_4U_4F_4$  coefficient of  $-0.04 \pm 0.03$  for this lowest temperature implies an internal field of  $320 \pm 130$  kG. (b) The lower limit—If no background corrections whatever are made (or if the background is assumed to have the same angular distribution as the 920-keV peak), the fields required to fit the data fall between 300 and 400 kG. Taking into account all the possible sources of error, a field of 250 kG for Ag in Fe seems a conservative lower limit.

With these limits, we suggest  $350 \pm 100$  kG as a tentative value for the magnitude of the hyperfine field at Ag

nuclei in Fe. It follows from the above  $\text{Ag}^{110m}$  results that the corresponding value for Ag in Ni is  $108 \pm 30$  kG. Because of experimental difficulties the  $\text{Ag}^{104}$   $\gamma$ -ray experiments are intrinsically of low accuracy. Rather than try to improve this accuracy slightly by further experiments in  $\text{Ag}^{104}$ , we prefer to determine the moment of  $\text{Ag}^{110m}$  by resonance methods and to obtain the internal fields by comparison of this moment with the hfs constants for  $\text{Ag}^{110m}$  in Fe and Ni. Such experiments are under way.

The main purpose of the  $\text{Ag}^{104}$  experiments was a sign determination of the hyperfine fields. This was easily done, with the results shown in Fig. 15. For a  $5+ (\beta^+) 4+$  transition, the coefficient of  $\cos\theta$  in Eq. (5) is positive; that is, positrons are preferentially emitted along the direction of the angular momentum vectors (i.e., along the polarization direction) of the parent nuclei. The higher intensity was observed with the small polarizing field at 180° from the counter direction. Thus the internal field must have oriented the nuclei *antiparallel* to the polarizing field. Since the nuclear moment is positive, it follows that the internal field was itself antiparallel to the external field, or *negative*. The tentative values for the internal fields now become

$$H_i = -(350 \pm 100) \text{ kG (Ag in Fe)},$$

$$H_i = -(108 \pm 30) \text{ kG (Ag in Ni)}.$$

It should be noted that the magnitudes of these fields are based on nuclear orientation experiments with an isotope of 1-h half-life, in an iron-palladium alloy. More reliable (and more accurate) values await a determination of the magnetic moment of  $\text{Ag}^{110m}$ .

#### D. Interpretation of the Internal Fields

The internal fields determined here can best be interpreted as part of a systematic discussion of induced internal fields. Such a discussion appears separately in the following paper. We note here that the field derived above for Ag in Fe is in good agreement with the value predicted<sup>4</sup> on the basis of the systematics,  $H = -400$  kG. The quantitative agreement must not be taken too seriously, because neither value is very accurate. Still the sign is negative, as predicted, and we conclude that the systematic correlation has some predictive value.

*Note added in proof.* Steven Schmelling has recently measured the magnetic moment of  $\text{Ag}^{110m}$  by atomic beam techniques, and has kindly communicated to us the preliminary result,  $\mu = +3.68$  nm. An error of 5% might be assigned to this value, to cover a possible hfs anomaly. Hyperfine fields for Ag in Fe and Ag in Ni are thus  $-272(19)$  and  $-84(5)$  kG, respectively.